The 2014 World Congress on
Advances in Civil, Environmental, and Materials Research (ACEM14)
Busan, Korea, August 24-28, 2014

Turbulence characteristics relative to moving vehicles

*Mengxue Wu[1b], Yongle Li[1a], Xinzhong Chen[2a], Peng Hu[1c]

[1] *Department of Bridge Engineering, Southwest Jiaotong University, Chengdu, Sichuan 610031, P. R. China*
[2] *Wind Science and Engineering Research Center, Department of Civil and Environmental Engineering, Texas Tech University, Lubbock, Texas 79409-1023, USA*

ABSTRACT

To investigate turbulence characteristics relative to moving vehicles under cross wind, based on Taylor's frozen turbulence hypothesis and isotropic turbulence model, formulations for calculating the power spectra of wind turbulence relative to moving vehicles are derived from the Kaimal spectrum of longitudinal wind fluctuation. The results can be applied for any vehicle moving direction, and for both longitudinal and lateral components of wind turbulence. In addition, the turbulence correlation characteristics with respect to moving vehicles are analyzed. The effects of speed ratio of vehicle speed to mean wind speed on the wind spectra and correlation characteristics are investigated. Both the increases in wind power spectrum and correlation contribute to larger aerodynamic forces and wind-induced vehicle vibration as the increasing speed ratio.

1. INTRODUCTION

As vehicle operating speed increases and mass decreases, the wind-induced traffic accidents due to strong crosswind have been common in the world (Diedrichs 2006; Gawthorpe 1994; Johnson 1996). The safety and comfort of running vehicles in strong crosswind conditions become one of the increasingly important factors (Baker 1991a, 1991b, 1991c and 2013). Currently, the time histories of random wind velocity fluctuations at finite discrete fixed-locations are generated with prescribed spectral characteristics (Cai and Chen 2004; Li et al. 2005; Xu and Guo 2003). However, when considering the effects of fluctuating wind on vehicles, the method to cope with the wind field of vehicles is to approximately take the wind fluctuations at the nearest fixed-locations. These approximate modeling of wind fluctuations on vehicles often causes discontinuity and may even introduce sudden changes in the wind fluctuations. Cooper (1984) calculated the power spectral density (PSD), cross-correlation and coherence of wind fluctuations normal to a moving vehicle using von Karman spectrum for wind turbulence at fixed-locations. Baker (1991b, 1991c and 2013) presented a

* Corresponding Author, Ph.D. Candidate, E-mail : mxswjtu@126.com
[a] Professor
[b] Ph.D. Candidate
[c] Ph.D.

comprehensive study on unsteady aerodynamic forces and dynamic response of vehicles in frequency, amplitude and time domains.

In present study, based on Taylor's frozen turbulence hypothesis (Taylor 1938) and isotropic turbulence model, formulations for calculating the power spectra of wind turbulence relative to moving vehicles are derived from the Kaimal spectrum of longitudinal wind fluctuation. In addition, the turbulence correlation characteristics with respect to moving vehicles are analyzed. The effects of speed ratio of vehicle speed to mean wind speed on the wind spectra and correlation characteristics are investigated.

2. WIND POWER SPECTRA RELATIVE TO MOVING VEHICLES

2.1 Kaimal spectrum of longitudinal wind fluctuation

The power spectral density (PSD) of *u*-component $S_u(n)$, is given as the Kaimal spectrum (Kaimal et al., 1972):

$$\frac{nS_u(n)}{u_*^2} = \frac{200\hat{n}}{(1+50\hat{n})^{5/3}} \tag{1}$$

where *n* is the frequency in Hz; $\hat{n} = nz/\overline{U}$ is the non-dimensional frequency; $\overline{U}$ is the mean wind velocity at the height *z* above the ground, u_* is the shear velocity of the flow. The standard deviation (STD) of *u*-component is then given as $\sigma_u = \sqrt{6}u_*$.

2.2 Taylor's frozen turbulence hypothesis

Based on Taylor’s frozen turbulence hypothesis, the wind fluctuations at two points along the mean wind speed direction are related as follows:

$$u(x,t) = u(x-\overline{U}t,0), \quad v(x,t) = v(x-\overline{U}t,0) \tag{2}$$

Taylor's hypothesis can be applied to turbulence except at large wavelengths (very low frequencies). The significant frequency range for ground vehicles is about 0.5 to 3.0 Hz, thus this hypothesis can be applied to study the unsteady aerodynamics of moving vehicles.

2.3 Auto-correlation coefficient functions at fixed points

The auto-correlation coefficient function at a stationary point can be obtained from the Kaimal longitudinal spectrum by Fourier transformation:

$$\rho_u(\tau) = \frac{1}{\sigma_u^2}\int_0^{+\infty} S_u(n)\cos(2\pi n\tau)dn = 1 - 0.036\tilde{r}^2 + 0.2\tilde{r}^{7/6} LommelS2\left(\frac{11}{6},\frac{1}{2},\frac{\pi}{25}\tilde{r}\right) \tag{3}$$

where $\tilde{r} = \tau\overline{U}/z$ is a non-dimensional variable; and $LommelS2(p,q,x)$ is a special function with three parameters, which is the second kind of solutions of equation $x^2y'' + xy' + (x^2 - q^2)y = x^{p+1}$ (Gradsbteyn and Ryzbik, 2000).

For the convenience of subsequent calculations, Eq. (3) is numerically fitted as the following formulation of non-dimensional variable $\tilde{r}$, i.e., $\rho_u(\tau) = f(\tilde{r})$.

$$f(\tilde{r}) = 0.013 + 0.467\exp(-\tilde{r}/4.296) + 0.201\exp(-\tilde{r}/0.797) + 0.281\exp(-\tilde{r}/15.742) \tag{4}$$

The auto-correlation coefficient function of lateral wind fluctuation, i.e., $\rho_v(\tau) = g(\tilde{r})$ can be obtained from the longitudinal auto-correlation coefficient function $\rho_u(\tau) = f(\tilde{r})$ under the assumption of isotropic turbulence (ESDU, 1985):

$$g(\tilde{r}) = f(\tilde{r}) + \frac{1}{2}\Delta r \frac{df(\tilde{r})}{d(\Delta r)} \tag{5}$$

where $\Delta r = \tau\overline{U}$.

Substituting Eq. (4) into Eq. (5), the lateral auto-correlation coefficient function can be expressed as:

$$\begin{aligned} g(\tilde{r}) &= 0.013 + (0.467 - 0.054\tilde{r})\exp(-\tilde{r}/4.296) + (0.201 - 0.126\tilde{r})\exp(-\tilde{r}/0.797) \\ &+ (0.281 - 0.009\tilde{r})\exp(-\tilde{r}/15.742) \end{aligned} \tag{6}$$

2.4 Cross-correlation coefficient functions relative to moving vehicles

Referring to Fig. 1, a vehicle is moving at a constant speed V along a straight line N-0 through the origin of the global coordinate system 0-XYZ, at an angle ϕ to the X-axis. The local coordinate system N-ξηζ (origin N) is fixed on the vehicle, with the plane N-η-ζ is close to the surface of the vehicle. The two physical points P and P' are fixed on the moving vehicle, and the local coordinates of P and P' are $(0,\eta,\zeta)$and $(0,\eta',\zeta')$, respectively. The position vectors $\vec{r}(t)$ of P and $\vec{r}'(t+\tau)$ of P' in the global coordinate system can be found. Applying Taylor's frozen turbulence hypothesis, an equivalent point P_e' in the frozen turbulence field (at time t) can be found corresponding to the physical point P' (at time t+τ), which is a distance $\tau\overline{U}$ away from point P' in the negative X-axis. The equivalent separations between points P and P_e' along the X, Y and Z axes in the frozen field are:

$$\Delta x_e = (\eta' - \eta - V\tau)\cos\phi - \tau\overline{U} \tag{7a}$$

$$\Delta y_e = (\eta' - \eta - V\tau)\sin\phi \tag{7b}$$

$$\Delta z = \zeta' - \zeta \tag{7c}$$

The expression form of the turbulence cross-correlation coefficient function relative to moving vehicles can be expressed as (Cooper, 1984):

$$\rho_{ij}^{M}(\vec{r},\vec{r}';\tau) = c_{ij} f(\tilde{r}) + (1 - c_{ij}) g(\tilde{r}) \tag{8}$$

where the superscript *M* represents that the vehicle motion is considered; $f(\tilde{r})$ and $g(\tilde{r})$ are the longitudinal and lateral auto-correlation coefficient functions, respectively; $\tilde{r} = \Delta r_e / z_m$; $\Delta r_e = \sqrt{\Delta x_e^2 + \Delta y_e^2 + \Delta z^2}$; $z_m = \frac{1}{2}(z + z')$; for *i*, *j* = *u*, $c_{uu} = (\Delta x_e / \Delta r_e)^2$; for *i*, *j* = *v*, $c_{vv} = (\Delta y_e / \Delta r_e)^2$; for *i* = *u*, *j* = *v*, $c_{uv} = \frac{\Delta x_e \cdot \Delta y_e}{\Delta r_e^2}$.

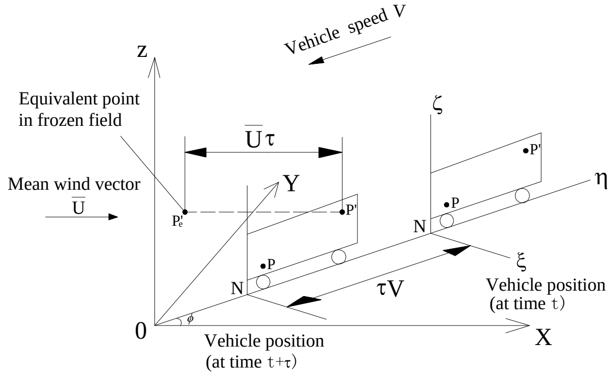

Fig. 1 Two points moving with the vehicle and equivalent point (Cooper, 1984)

2.5 power spectra of turbulence relative to moving vehicles

The auto-correlation coefficient function of turbulence at the moving point P can be readily obtained from Eq. (8) by setting the two points are identical, i.e., $\Delta x_e = -V\tau\cos\phi - \tau\overline{U}$, $\Delta y_e = -V\tau\sin\phi$, and $\Delta z = 0$. The power spectra of *i*-component (*i* = *u*, *v*) can be given as:

$$S_i^M(n) = \sigma_i^2 \int_0^{+\infty} \rho_i^M(\tau)\cos(2\pi n\tau)d\tau = 4u_*^2 \cdot \frac{z}{V_r} \cdot \sqrt{\frac{\pi}{2}}\left[d_i \cdot A + (1 - d_i)(A - B - C - D)\right] \tag{9}$$

where

for *i* = *u*,

$$d_u = \left[(\overline{U} + V\cos\phi)/V_r\right]^2 \tag{9a}$$

for *i* = *v*,

$$d_v = \left[(V\sin\phi)/V_r\right]^2 \tag{9b}$$

$$V_r = \sqrt{\overline{U}^2 + V^2 + 2\overline{U}V\cos\phi} \tag{9c}$$

$$A = \frac{0.52017}{0.05419 + s^2} + \frac{1.20867}{1.57290 + s^2} + \frac{0.08540}{0.00404 + s^2} \tag{9d}$$

$$B = \frac{0.01409(1 - 18.45244 s^2)}{(0.05419 + s^2)^2} \tag{9e}$$

$$C = \frac{0.95056(1 - 0.63577s^2)}{(1.57290 + s^2)^2} \tag{9f}$$

$$D = \frac{0.00017(1 - 247.81938s^2)}{(0.00404 + s^2)^2} \tag{9g}$$

$$s = 2\pi\hat{n} \tag{9h}$$

$$\hat{n} = nz / V_r \tag{9i}$$

It can be readily illustrated that when the vehicle is stationary ($V = 0$), the above wind spetra relative to moving vehicles reduce to those at fixed points, seen Fig. 2.

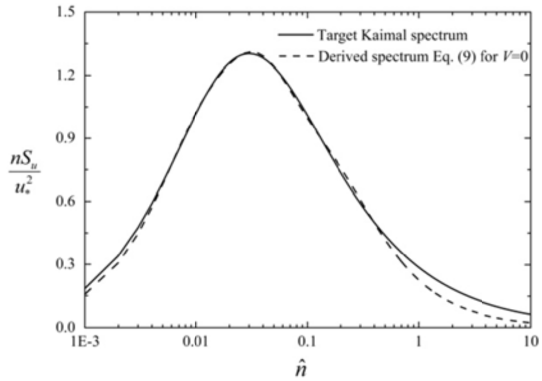

Fig. 2 The comparison of target Kaimal spectrum and derived spectrum

3. THE EFFECTS OF SPEED RATIO ON WIND CHARACTERISTICS

3.1 Wind power spectra

Fig.3 displays the influence of speed ratio on the spectra of *u*- and *v*-components of wind fluctuation, where the wind direction is normal to the moving vehicle, i.e., $\phi = 90^\circ$. It is seen that the spectrum shifts into higher frequencies. As a result, the energy in the range 0.2-4.0Hz increases with increasing speed ratio. This is important to ground vehicles which have a significant frequency range from 0.5Hz to 3.0Hz. It indicates that the effect of movement is to make the moving vehicle experience higher wind energy at the frequency range of interest, thus leads to higher aerodynamic forces.

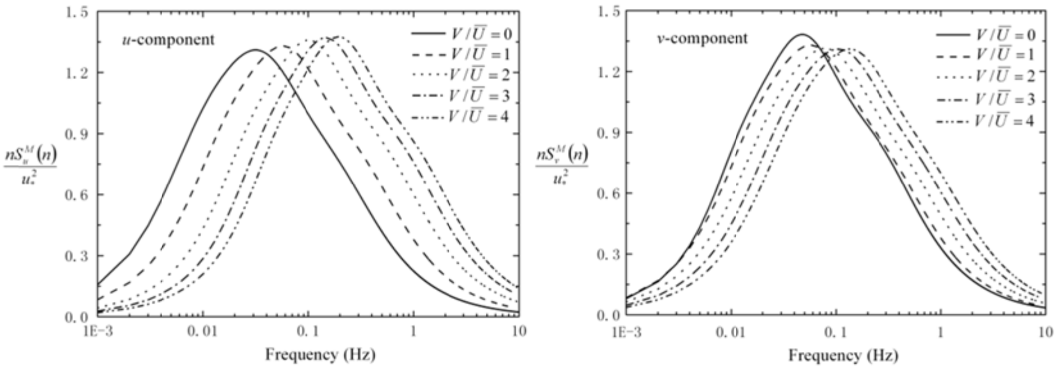

Fig.3 The influence of speed ratio on power spectra of *u*- and *v*-components

3.2 Auto-correlation coefficient function and turbulence length scale

Fig.4 displays the longitudinal auto-correlation coefficient function at different speed ratios where $\phi = 90^{\circ}$. The normalized non-dimensional time variable is defined as $\tilde{\tau} = \tau V_r / z$. The integrations of these autocorrelation coefficients give the corresponding turbulence length scale. It is observed that the length scale 'seen' from the moving vehicle decreases with increasing speed ratio. It indicates that compared with the stationary case, the motion of vehicle results in reducing the time of vehicle passing by the turbulent eddies, corresponding to the reduction of the average size of turbulent eddies 'seen' from the moving vehicle. In addition, it should be noted that the sensitivity of the auto-correlation coefficient function to the speed ratio reduces with increasing speed ratio.

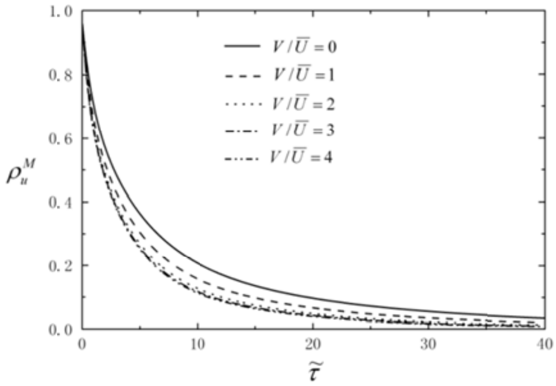

Fig.4 The longitudinal auto-correlation coefficient function at different speed ratios

3.3 Cross-correlation coefficient function

Fig.5 shows the cross-correlation coefficient function of *u*-component of wind fluctuation for different non-dimensional separation distance $\tilde{d} = (\eta' - \eta)/z$ and different speed ratios $V/\overline{U} = 1$ and 4, where $\zeta' = \zeta$. The wind direction is normal to the moving vehicle, i.e., $\phi = 90^{\circ}$. With consideration of vehicle motion, it can be seen that the turbulence cross-correlation coefficient rise to a maximum value at some value of the time delay, which is a function of the separation distance and speed ratio.

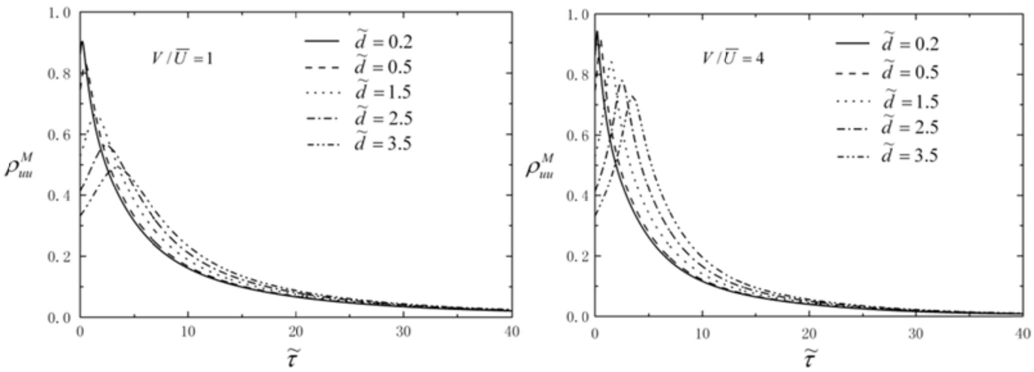

Fig.5 Cross-correlation coefficient function relative to moving vehicles

4. CONCLUSIONS

The power spectra and correlation coefficient functions of wind turbulence relative to moving vehicles were deduced based on the basis of Taylor's frozen turbulence hypothesis and isotropic turbulence model. The results can be applied for any vehicle moving direction, and for both longitudinal and lateral components of wind turbulence. The results showed that the moving vehicles experience higher wind energy at the frequency range of interest, thus leads to higher aerodynamic forces. The motion of vehicle resulted in reducing the time of vehicle passing by the turbulent eddies, corresponding to the reduction of the average size of turbulent eddies 'seen' from the moving vehicle. That suggested that the wind fluctuations and thus the aerodynamic forces on moving vehicles were more correlated in space. Both the increases in power spectrum and correlation contributed to larger aerodynamic forces and wind-induced vehicle vibration as the increasing speed ratio.

Acknowledgements

The authors are grateful for the financial supports from the National Natural Science Foundation of China under Grant NNSF-U1334201, and the Major State Basic Research Development Program of China (973 Program) (Project No. 2013CB036206).

REFERENCES

Baker, C.J. (1991a), "Ground vehicles in high cross winds Part I: Steady aerodynamic forces", *J. Fluids Struct.*, **5**, 69-90.
Baker, C.J. (1991b), "Ground vehicles in high cross winds Part II: Unsteady aerodynamic forces", *J. Fluids Struct.*, **5**, 91-111.
Baker, C.J. (1991c), "Ground vehicles in high cross winds Part III: The interaction of aerodynamic forces and the vehicle system", *J. Fluids Struct.*, **5**, 221-241.
Baker, C.J. (2013), "A framework for the consideration of the effects of crosswinds on trains", *J. Wind Eng. Ind. Aerodyn.*, **123**, 130-142.
Cai, C.S. and Chen, S.R. (2004), "Framework of vehicle–bridge–wind dynamic analysis", *J. Wind Eng. Ind. Aerodyn.*, **92**, 579-607.
Cooper, R.K. (1984), "Atmospheric turbulence with respect to moving ground vehicles", *J. Wind Eng. Ind. Aerodyn.*, **17**, 215-238.
Diedrichs, B. (2006), "Studies of two aerodynamics effects on high-speed trains crosswind stability and discomforting car body vibrations inside tunnels", Ph.D. Thesis, Aeronautical and Vehicle Engineering, Royal Institute of Technology.
ESDU. (1985), "Characteristics of atmospheric turbulence near the ground. Part II: single point data for strong winds (neutral atmosphere)", Item No. 85020, Engineering Sciences Data Unit, London.
Gawthorpe, R.G. (1994), "Wind effects on ground transportation", *J. Wind Eng. Ind. Aerodyn.*, **52**, 73-92.
Gradsbteyn, I.S. and Ryzbik, L.M. (2000), *Table of integrals, series and products*, 6th ed. Academic Press, New York.
Johnson, T. (1996), "Strong wind effects on railway operations-16th October 1987", *J.*

Wind Eng. Ind. Aerodyn., **60**, 251-266.

Kaimal, J.C., Wyngaard, J.C., Izumi, Y. and Cote, O.R. (1972), “Spectral characteristics of surface-layer turbulence”, *Quart. J. R. Met. Soc.*, **98**, 563-589.

Li, Y.L., Qiang, S.Z., Liao H.L. and Xu, Y.L. (2005), “Dynamics of wind-rail vehicle-bridge systems”, *J. Wind Eng. Ind. Aerodyn.*, **93**, 483-507.

Taylor, G.I. (1938), “The spectrum of turbulence”, *Proceedings of the Royal Society*, London, **A164**, 476-490.

Xu, Y.L. and Guo, W.H. (2003), “Dynamic analysis of coupled road vehicle and cable-stayed bridge systems under turbulent wind”, *Eng. Struct*., **25**, 473-486.